

<sup>1</sup>Key Laboratory for Water and Sediment Sciences, Ministry of Education, College of Environmental Sciences and Engineering, Peking University, Beijing 100871, China; <sup>2</sup>State Environmental Protection Key Laboratory of All Materials Fluxes in River Ecosystems, Ministry of Ecology and Environment, Beijing 100871, China; <sup>3</sup>Laboratoire des Sciences du Climat et de l'Environnement, Institut Pierre Simon Laplace, Commissariat à l'Énergie Atomique et aux Énergies Alternatives, CNRS, Université de Versailles Saint-Quentin-en-Yvelines, Gif-sur-Yvette 91191, France; <sup>4</sup>Key Laboratory of Reservoir Environment, Chongqing Institute of Green and Intelligent Technology, Chinese Academy of Sciences, Chongqing 400714, China; <sup>5</sup>State Key Laboratory of Water Resources and Hydropower Engineering Science, Wuhan University, Wuhan 430072, China; <sup>6</sup>Department of Water Environment, China Institute of Water Resources and Hydropower Research, Beijing 100038, China; <sup>7</sup>MOE Key Laboratory of Regional Energy Systems Optimization, Resources and Environmental Research Academy, North China Electric Power University, Beijing 102206, China and <sup>8</sup>School of Engineering, The University of Edinburgh, Edinburgh EH9 3JL, UK

## EARTH SCIENCES

## Three Gorges Dam: friend or foe of riverine greenhouse gases?

Jinren Ni<sup>1,2,\*</sup>, Haizhen Wang<sup>1</sup>, Tao Ma<sup>1</sup>, Rong Huang<sup>1</sup>, Philippe Ciais<sup>3</sup>, Zhe Li<sup>4</sup>, Yao Yue<sup>5</sup>, Jinfeng Chen<sup>1</sup>, Bin Li<sup>1</sup>, Yuchun Wang<sup>6</sup>, Maosheng Zheng<sup>7</sup>, Ting Wang<sup>1</sup> and Alistair G.L. Borthwick<sup>8</sup>

### ABSTRACT

Dams are often regarded as greenhouse gas (GHG) emitters. However, our study indicated that the world's largest dam, the Three Gorges Dam (TGD), has caused significant drops in annual average emissions of CO<sub>2</sub>, CH<sub>4</sub> and N<sub>2</sub>O over 4300 km along the Yangtze River, accompanied by remarkable reductions in the annual export of CO<sub>2</sub> (79%), CH<sub>4</sub> (50%) and N<sub>2</sub>O (9%) to the sea. Since the commencement of its operation in 2003, the TGD has altered the carbonate equilibrium in the reservoir area, enhanced methanogenesis in the upstream, and restrained methanogenesis and denitrification via modifying anoxic habitats through long-distance scouring in the downstream. These findings suggest that 'large-dam effects' are far beyond our previous understanding spatiotemporally, which highlights the fundamental importance of whole-system budgeting of GHGs under the profound impacts of huge dams.

**Keywords:** Three Gorges Dam, greenhouse gas, spatiotemporal variation, equilibrium, Yangtze River, whole system analysis

### INTRODUCTION

Most rivers worldwide are supersaturated with greenhouse gases (GHGs) owing to inputs of carbon (C) and nitrogen (N) from land, and become net sources of GHGs for the atmosphere [1]. To meet the growing global demand for water and energy, more than 70 000 large dams have been constructed [2]. Such dams are regarded as a source of excessive GHG emissions [3–5]. The estimated annual emissions are 48 Tg C as CO<sub>2</sub> and 3 Tg C as CH<sub>4</sub> from global hydropower reservoirs, and 0.03 Tg N as N<sub>2</sub>O from all reservoirs in the world [4,6].

Previous studies on the effects of dams on GHGs have been mostly limited to the vicinity of reservoirs [7–10]. Although these considerations hold for small dams (reservoir capacity < 10 km<sup>3</sup>), the impact of large dams on GHGs (reservoir capacity ≥ 10 km<sup>3</sup>) is much greater because the original physical and biochemical equilibria are disrupted over large spatiotemporal scales. Firstly, a large dam alters the hydrodynamic conditions and material fluxes of a river: after operation commences, the

peak flood discharge decreases and fluxes of nutrients and sediments exported to the sea are often reduced [11–14]. Secondly, the river regime tends to remain stable, but increasing longitudinal erosion of the riverbed beyond the dam causes long-term readjustment over a considerable distance [15]. Thirdly, changes to water and sediment fluxes significantly affect the functioning of microbial communities [16–18] (e.g. photosynthesis, methanogenesis and denitrification) and GHG emissions (Supplementary Table 1).

As the world's largest dam, the Three Gorges Dam (TGD) has been regarded as a significant source of GHG emissions [3,4,19]. For example, CO<sub>2</sub> and CH<sub>4</sub> emissions from the 25 km<sup>2</sup> core reservoir area upstream of the TGD in 2008 were estimated to be 40 and 20 Gg yr<sup>-1</sup>, respectively, ~40- and 20-fold larger than before impoundment [20]. Similar findings [4,21] reported that the total CH<sub>4</sub> emission rate in the Three Gorges Reservoir (TGR) was 0.315 Gg yr<sup>-1</sup>. However, the impact of the TGD extends far beyond the reservoir area. The TGD has

\*Corresponding author. E-mail: [jinrenni@pku.edu.cn](mailto:jinrenni@pku.edu.cn)

Received 17 November 2021; Revised 2 January 2022; Accepted 17 January 2022

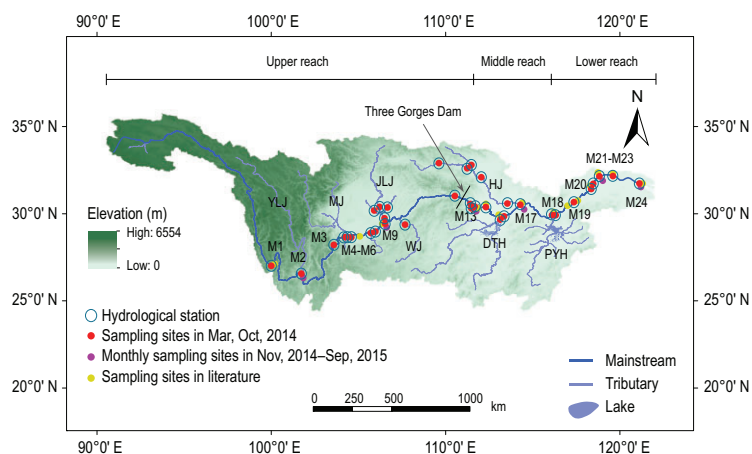


**Figure 1.** The Yangtze River Basin and sampling sites. Lines indicate the mainstream river and its tributaries, the former having a length of 4300 km (i.e. the actual sinuous channel length, equivalent to 2.05 times the straight-line distance of 2102 km from the start to the end of the sampling sites). Yellow solid circles show the locations of previous sampling sites (see Supplementary Tables 2–3); red solid circles show the locations of our recent simultaneous sampling sites in March and October 2014 (for details see Supplementary Table 4); purple solid circles show the locations of our monthly sampling sites from October 2014 to September 2015; blue open circles show the locations of the hydrological stations. The upper reach is from Shigu (M1) to Yichang (M13), the middle reach from Yichang to Hukou (M18) and the lower reach from Hukou to Xuliujing (M24). The major tributaries include Yalongjiang (YLJ), Minjiang (MJ), Jialingjiang (JLJ), Wujiang (WJ) and Hanjiang (HJ); two river-regulated lakes are Dongting (DTH) and Poyang (PYH).

altered hydrodynamic conditions along almost the entire length of the Yangtze, as physical and biochemical processes have readjusted both upstream and downstream of the dam, most notably the long-distance, long-term scouring of the riverbed downstream of the dam [15,22,23]. This highlights the necessity of whole-river analysis in order to properly assess the changes in GHG fluxes caused by large dams.

Here, we estimate changes in dissolved and emitted fluxes of GHGs in the Yangtze River before and after the TGD became operational in 2003. Based on the time series of 30 water quality indices monitored over 312 months (1990–2015) and the measured GHGs (Supplementary Tables 2–4) along 4300 km of the Yangtze River (Fig. 1), CO<sub>2</sub> is calculated using the well-known CO<sub>2</sub>SYN model, while CH<sub>4</sub> and N<sub>2</sub>O are estimated with artificial neural networks (ANNs; see Methods).

## RESULTS AND DISCUSSION

### Temporal effect of the TGD on CO<sub>2</sub> fluxes

The mean annual *p*CO<sub>2</sub> between 1990 and 2002 was 2526 μatm (Fig. 2). Subsequently, *p*CO<sub>2</sub> declined greatly to 1336 μatm once the TGD began operation over the whole mainstream (Fig. 2a). This de-

clining trend is particularly significant in the middle and lower reaches, though annual *p*CO<sub>2</sub> in the upper reach remained relatively steady before and after 2003 (Fig. 2b–d). The spatially averaged annual *p*CO<sub>2</sub> was 2205<sup>+2497</sup><sub>−925</sub> μatm (where the numbers display the mean and range of values) in the middle reach. *p*CO<sub>2</sub> increased to 2974 μatm during the 1990s, peaked in 1996 and declined significantly to 1720 μatm after TGD impoundment [24] (Fig. 2c). In the middle reach, *p*CO<sub>2</sub> decreased from 2907 to 1446 μatm in the wet season and from 2196 to 1377 μatm in the dry season (Supplementary Fig. 1a–d).

From 1990 to 2015, CO<sub>2</sub> exported to the East China Sea exhibited substantial inter-annual variations (Supplementary Fig. 2). The mean annual value increased from ~469 Gg C yr<sup>−1</sup> in 1993 and reached a peak of 3354 Gg C yr<sup>−1</sup> during the 1998 flood before declining to pre-1993 levels by 2003 (Supplementary Fig. 2). The mean exported CO<sub>2</sub> flux from 1991 to 2015 was 1128 Gg C yr<sup>−1</sup>, corresponding to 5.6% of dissolved inorganic carbon transported by the Yangtze River (Supplementary Table 5). The annual averaged CO<sub>2</sub> outgassing flux and CO<sub>2</sub> exported to the sea over the Yangtze experienced remarkable drops of 55% and 79% since 2003, suggesting a much stronger effect, due to TGD impoundment, on *p*CO<sub>2</sub> than that from other influencing factors (such as the anthropogenic discharge of sulfur and nitrogen containing pollutants) reported previously [24].

Monthly and annual CO<sub>2</sub> emission fluxes from the upper, middle and lower reaches were on average lower after 2003 than before, indicating that the entire mainstream progressively became a smaller emission source (Supplementary Fig. 3). The largest change occurred in the middle and lower reaches, where CO<sub>2</sub> emission flux dropped from 2723 Gg C yr<sup>−1</sup> before TGR impoundment to 1087 Gg C yr<sup>−1</sup> after. Annual averaged CO<sub>2</sub> emission flux from the Yangtze mainstream was estimated as 2420<sup>+2590</sup><sub>−1200</sub> Gg C yr<sup>−1</sup> (Supplementary Table 6), which accounts for emissions from 1.3% of global rivers and 4.8% of temperate rivers [1,25] between 25°N and 50°N. These results were convincing with uncertainty analysis based on representative stations as described in the Supplementary Data.

### Temporal effect of the TGD on CH<sub>4</sub> fluxes

To estimate dissolved and emitted CH<sub>4</sub> over the Yangtze River before and after impoundment of the TGR, monthly observed data of chemical oxygen demand, dissolved oxygen, water temperature, pH and nitrogen during 1990–2015 were used for validation and verification as input variables of ANN

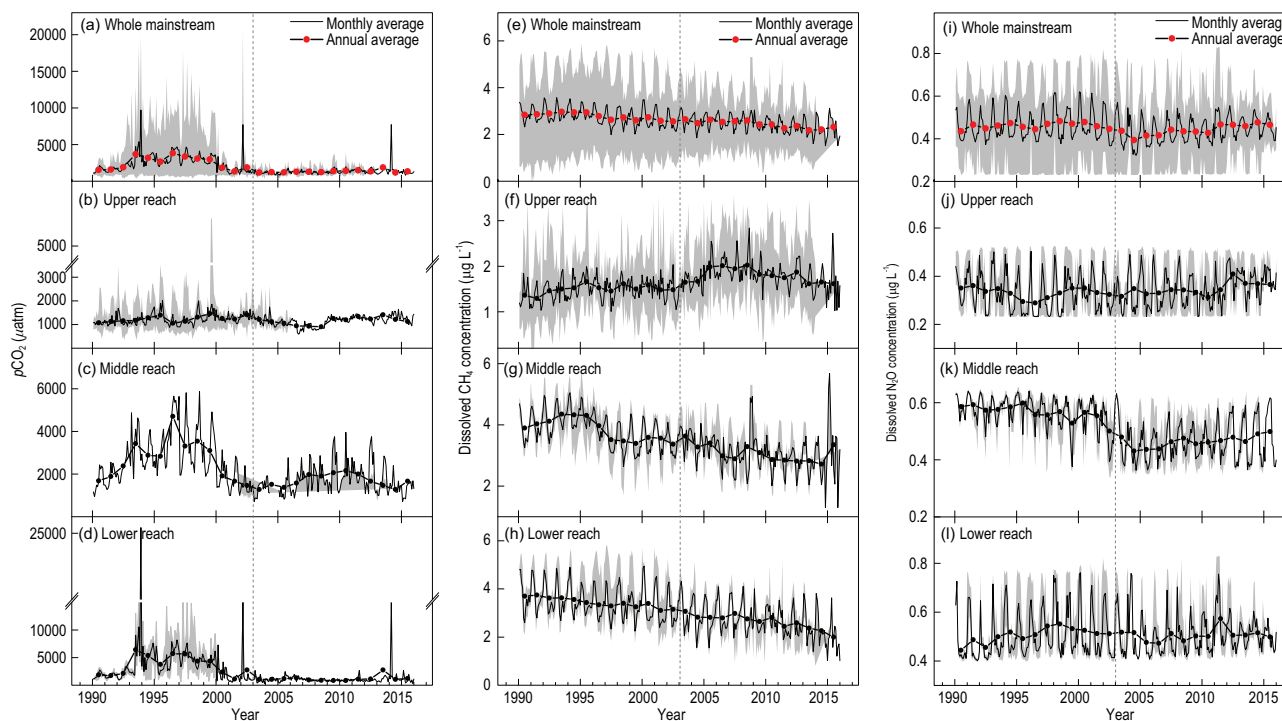


**Figure 2.** Temporal variations in monthly and annual averages of dissolved-GHG concentrations from 1990 to 2015: (a–d)  $p\text{CO}_2$ , (e–h) dissolved  $\text{CH}_4$ , and (i–l) dissolved  $\text{N}_2\text{O}$ . The shadow areas represent the range of dissolved-GHG concentrations at different monitoring stations in the corresponding reaches. Vertical dashed lines denote 2003, when the TGD commenced operation.

models (see Methods). Supplementary Fig. 4 shows spatiotemporal variations in dissolved nitrogen ( $\text{NH}_4^+$ ,  $\text{NO}_3^-$ ,  $\text{NO}_2^-$ ) in the whole mainstream during the period 1990–2015.

After the TGR impoundment in 2003, both dissolved and emitted  $\text{CH}_4$  concentrations increased in the upper reach, decreased in the middle reach and hardly changed in the lower reach (Fig. 2f–h, Supplementary Fig. 5b–d). The annual averaged  $\text{CH}_4$  concentration from 1990 to 2015 over the whole mainstream was  $2.22^{+0.54}_{-0.65} \mu\text{g L}^{-1}$  (Fig. 2e), comparable to that for the Amazon River (Supplementary Table 7) [26]. The mean dissolved  $\text{CH}_4$  was  $3.15^{+0.62}_{-0.56} \mu\text{g L}^{-1}$  in the dry season and  $2.57^{+0.59}_{-0.72} \mu\text{g L}^{-1}$  in the wet season in the Yangtze (Supplementary Fig. 1). A major change in seasonal cycles of dissolved  $\text{CH}_4$  occurred in 2003. In the wet season, the mean dissolved  $\text{CH}_4$  increased from 1.45 to 1.95  $\mu\text{g L}^{-1}$  in the upper reach but decreased from 3.51 to 3.02  $\mu\text{g L}^{-1}$  in the middle reach. Based on the parameters derived from representative stations (Supplementary Table 8), temporal variation in  $\text{CH}_4$  flux exported to the East China Sea decreased from 3.1 to 1.5  $\text{Gg C yr}^{-1}$  after 2003 (Supplementary Fig. 6). Emitted  $\text{CH}_4$  flux decreased from 3.3 to 2.7  $\text{Gg C yr}^{-1}$  along the whole mainstream, having increased from 0.4 to 0.5  $\text{Gg C yr}^{-1}$  upstream of the dam and decreased from 2.9 to 2.2  $\text{Gg C yr}^{-1}$

downstream of the dam since the operation of the TGD (Supplementary Fig. 7).

### Temporal effect of the TGD on $\text{N}_2\text{O}$ fluxes

Input variables in the ANN model for estimation of  $\text{N}_2\text{O}$  emissions included dissolved oxygen, water temperature, pH and nitrogen. Total dissolved nitrogen ( $\text{NH}_4^+ + \text{NO}_3^- + \text{NO}_2^-$ ) increased during the period of interest, while  $\text{NH}_4^+$  and  $\text{NO}_2^-$  had much lower concentration levels than  $\text{NO}_3^-$  (Supplementary Fig. 4). This is consistent with increasing nitrogen input from fertilizers to the Yangtze River basin in the past few decades, enhanced by population and economic growth in central and east China [27,28]. After training and verification of the ANN, the modeled results showed a slight reduction of dissolved and emitted  $\text{N}_2\text{O}$  owing to the dam’s operation since 2003. Over the Yangtze mainstream, the annual average concentration was  $0.45^{+0.38}_{-0.22} \mu\text{g L}^{-1}$  (Fig. 2i), demonstrating a moderate dissolved  $\text{N}_2\text{O}$  concentration compared with other large rivers (Supplementary Table 9). Dissolved  $\text{N}_2\text{O}$  reached a maximum of 0.55  $\mu\text{g L}^{-1}$  at the Xuliujing station in the river mouth (Fig. 2l), and a minimum of 0.32  $\mu\text{g L}^{-1}$  at the Luzhou station in the upper reach (Fig. 2j). Impoundment of

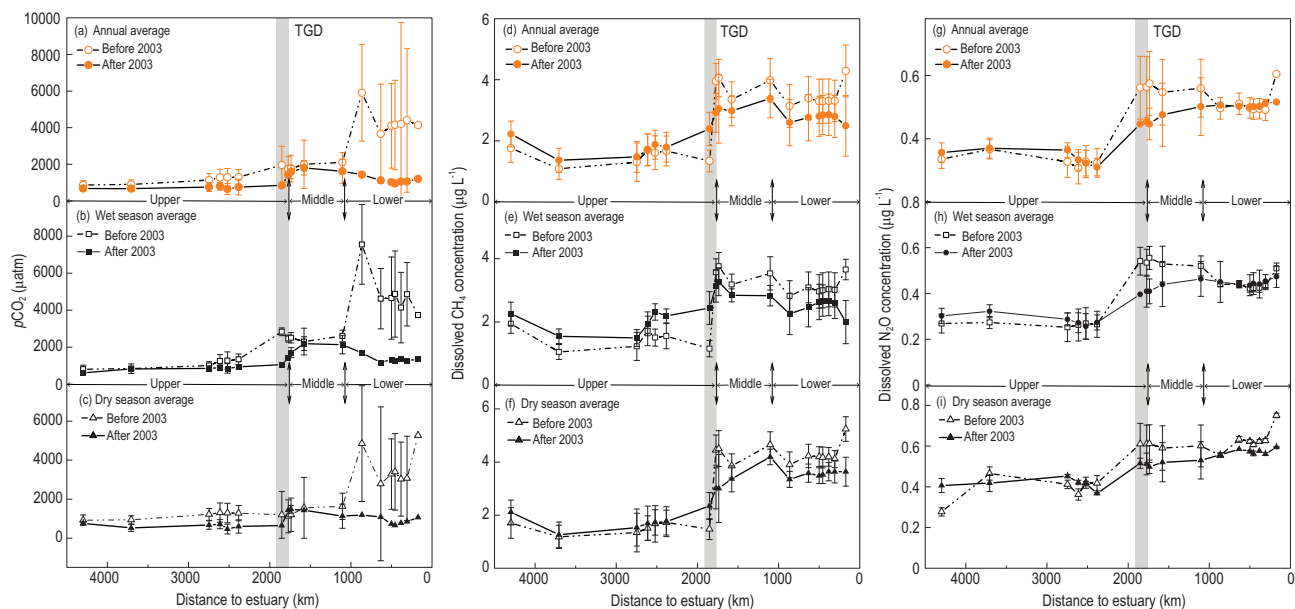


**Figure 3.** Spatial variations in annual and seasonal dissolved-GHG concentrations in the 4300-km stretch of the Yangtze River: (a–c) dissolved- $\text{CO}_2$  concentration, (d–f) dissolved  $\text{CH}_4$  concentration, and (g–i) dissolved  $\text{N}_2\text{O}$  concentration. The error bars are the annual standard deviations at the given monitoring stations. The shaded area indicates where the TGD reservoir is located.

the TGR operation caused dissolved  $\text{N}_2\text{O}$  to decrease from  $0.56$  to  $0.46 \mu\text{g L}^{-1}$  in the middle reach after 2003 (Fig. 2k). Large amplitude variations in seasonal  $\text{N}_2\text{O}$  patterns also occurred in the middle reach (Supplementary Fig. 1k). After 2003, the average dissolved  $\text{N}_2\text{O}$  concentration declined from  $0.61$  to  $0.51 \mu\text{g L}^{-1}$  in the dry season and from  $0.54$  to  $0.41 \mu\text{g L}^{-1}$  in the wet season in the middle reach. Seasonal differences of  $\text{N}_2\text{O}$  emission rates were also calculated (Supplementary Fig. 8e–h). The long-term average (1990–2015) displayed higher  $\text{N}_2\text{O}$  emission rates at Yichang and Wuhan in the wet season than in the dry season, in all cases indicating the Yangtze was a net source of  $\text{N}_2\text{O}$  (Supplementary Fig. 8). Meanwhile,  $\text{N}_2\text{O}$  emission rates at Yichang have fallen from  $39.3$  to  $19.2 \mu\text{g m}^{-2} \text{h}^{-1}$  during the wet season and from  $18.4$  to  $11.6 \mu\text{g m}^{-2} \text{h}^{-1}$  during the dry season (Supplementary Fig. 8g). Based on monthly dissolved  $\text{N}_2\text{O}$  and flow discharge, the highest values of  $\text{N}_2\text{O}$  fluxes to the estuary occurred in 1998, the year with historical floods. Mean annual dissolved  $\text{N}_2\text{O}$  fluxes to the estuary decreased from  $0.46$  to  $0.41 \text{ Gg N yr}^{-1}$  after TGD impoundment in 2003 (Supplementary Fig. 9), because of the disruptive effect on the physical and biochemical equilibria of the river. The annual  $\text{N}_2\text{O}$  outgassing in the mainstream was estimated as  $0.43 \text{ Gg N yr}^{-1}$  (Supplementary Fig. 10).

### Spatial effect of the TGD on GHG emissions

Before 2003,  $p\text{CO}_2$  ranged from  $880$  to  $4399 \mu\text{atm}$  in the mainstream channel of the Yangtze River (Fig. 3a). A trend of increasing  $p\text{CO}_2$  was evident along the mainstream, rising from  $1314 \mu\text{atm}$  in the upper reach to  $4111 \mu\text{atm}$  in the lower reach, along with the decreasing pH level of the lower reach and dilution by water entering from Poyang Lake during the period 1990–2002. After 2003,  $p\text{CO}_2$  was almost constant upstream of the TGD, but rose immediately downstream of the dam, affected by flow regulation and sediment trapping [29]. It has been estimated that reservoir sedimentation caused by the presence of a dam results in an average carbon accumulation rate of  $400 \text{ g m}^{-2} \text{ yr}^{-1}$  globally [30]. Carbon burial therefore results in a potential available carbon source for biological respiration and might increase  $p\text{CO}_2$  in a reservoir, particularly in the early years after impoundment [31]. Other human activities might also increase exchanges between water and mineral, thus increasing  $p\text{CO}_2$  [32]. Similar trends of increasing  $p\text{CO}_2$  were observed along the mainstream in both wet and dry seasons (Fig. 3b–c). The higher values of  $p\text{CO}_2$  in the wet season compared to the dry season, especially in middle and lower reaches, might be due to the efficient production of soil-originated  $\text{CO}_2$

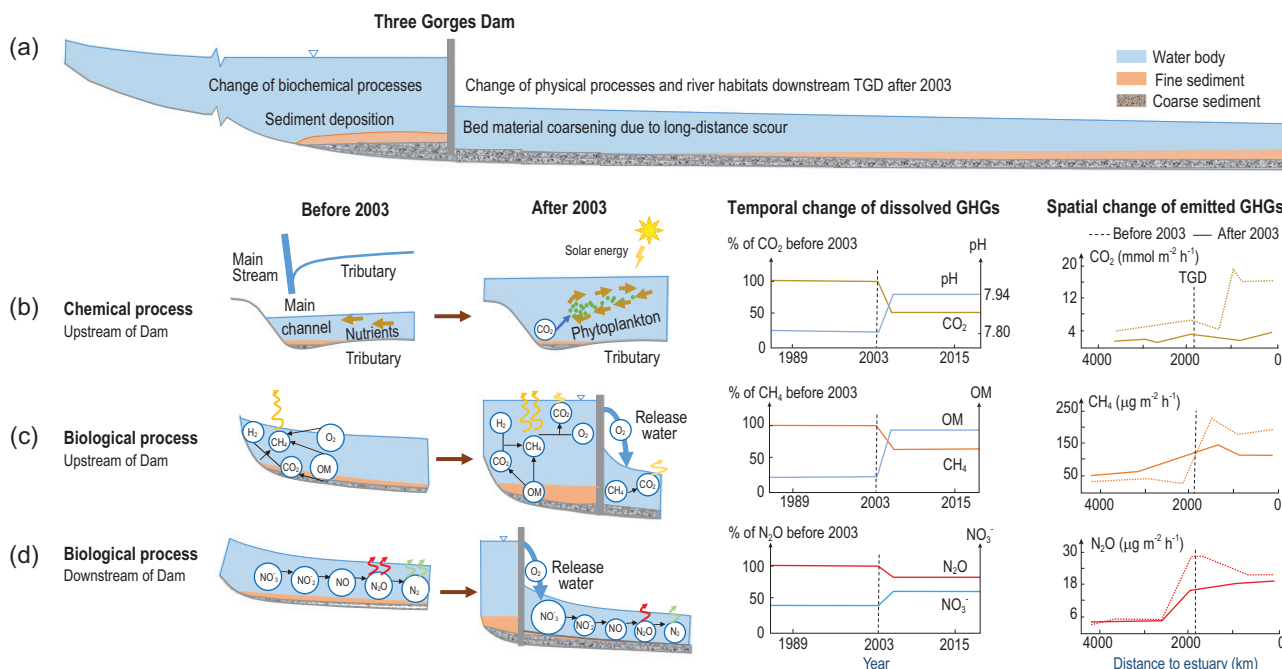


**Figure 4.** (a–d) Whole-system analysis concerning readjustment of physical and biogeochemical equilibria involved in the regulation effects of the TGD on GHG emissions from the Yangtze River.

and its transportation by surface run-off [31]. Supplementary Fig. 11 shows the CO<sub>2</sub> emission rate profiles along the mainstream before and after operation of the TGD. These are qualitatively very similar to the dissolved CO<sub>2</sub> profiles. After 2003, the mean CO<sub>2</sub> emission rate along the mainstream was  $3.0 \pm 1.7 \text{ mmol m}^{-2} \text{ h}^{-1}$ . Degassing rates were higher in the middle and lower reaches than in the upper reach, controlled by *p*CO<sub>2</sub>.

CH<sub>4</sub> concentration was lowest in the upper reach of the Yangtze in both wet and dry seasons (Fig. 3d–f), primarily because of lower levels of organic matter. After 2003, CH<sub>4</sub> concentration increased slightly from 1.50 to 1.83 μg L<sup>-1</sup> in the upper reach, and decreased from 3.13 to 2.74 μg L<sup>-1</sup> in the lower reach (Fig. 3d). The TGD impoundment influenced the CH<sub>4</sub> emission rate in a trend similar to that of its dissolved concentration (see Supplementary Fig. 5).

The TGD influenced N<sub>2</sub>O distributions both upstream and downstream of the dam, especially in the middle reach of the Yangtze (Fig. 3g). After 2003, annual averaged N<sub>2</sub>O concentrations decreased slightly from 0.42 to 0.38 μg L<sup>-1</sup> in the wet season and from 0.55 to 0.50 μg L<sup>-1</sup> in the dry season (Fig. 3h–i). The most remarkable decrease in N<sub>2</sub>O concentration occurred at Yichang, immediately downstream of the TGD (Supplementary Fig. 12a). At Yichang, monthly averaged N<sub>2</sub>O emission rates fell both in the wet and dry seasons, and the amplitude of the fluctuations in N<sub>2</sub>O emission rate also declined (Supplementary Fig. 12a) with smaller

seasonal differences (Supplementary Fig. 12b) after TGD impoundment.

### GHG fluxes in response to readjustment of physical and biochemical equilibria

Our study indicated that the TGD has caused significant drops in the overall annual GHG fluxes emitted to the atmosphere and exported to the sea since 2003 (Supplementary Table 10). To interpret such changes, a whole-river analysis (Fig. 4) must be made of the readjustments to hydrodynamic conditions (Fig. 4a) and biogeochemical equilibria (Fig. 4b–d) over the broader spatiotemporal scale of the river.

#### Cause of CO<sub>2</sub> drop

Due to TGD impoundment, a backwater zone developed upstream of the dam wherein water exchanges took place between the mainstream and tributaries (Fig. 4b). Water retention time significantly increased in the reservoir in addition to the significantly decreased flow velocity (<0.2 m s<sup>-1</sup>) in some tributaries entering into the reservoir. Such changes replenish nutrients in the tributaries via circulation with the mainstream [33]. Accumulated nutrients and restricted vertical mixing in the backwater area of the tributaries favored phytoplankton growth [34,35], causing algae to flourish [36] (Supplementary Table 11). Algae's

photosynthetic removal of  $\text{CO}_2$  and bioaccumulation of  $\text{NO}_3^-$ ,  $\text{H}_2\text{PO}_4^-$ ,  $\text{HPO}_4^{2-}$  and  $\text{PO}_4^{3-}$  resulted in a higher pH in the tributaries, promoting acceleration of eutrophication [37,38]. The higher pH in the tributaries helped neutralize hydrogen ions in the mainstream, breaking the carbonate equilibrium of the river and ultimately leading to a sharp drop in  $\text{CO}_2$  in the mainstream (Supplementary Fig. 13).

### Cause of $\text{CH}_4$ drop

Although  $\text{CH}_4$  increased upstream, a net reduction of  $\text{CH}_4$  emissions ( $\sim 17\%$ ) happened along the whole mainstream after the TGR impoundment, due to a decrease in  $\text{CH}_4$  downstream of the TGD. The input of dissolved  $\text{CH}_4$  into the ocean decreased by 50%, primarily because the TGD modified the GHG regime and disrupted the biotic equilibrium of the Yangtze (Fig. 4c). Upstream of the TGD, both dissolved and emitted  $\text{CH}_4$  increased after the reservoir impoundment, owing to the effects of flow regulation and sediment trapping. Such carbon burial promotes heterotrophic methanogenesis, thus increasing the dissolved  $\text{CH}_4$  content of the reservoir [29]. Anoxic conditions due to increased water depth in front of the dam would also be beneficial to methanogens locally [11]. However, both dissolved and emitted  $\text{CH}_4$  declined downstream of the dam, mainly because of riverbed scouring, which damaged the habitat of anaerobic *Archaea* responsible for heterotrophic methanogenesis [39,40]. In addition, the pre-impoundment clearance also reduced decomposition of organic carbon and inhibited the significant increase in  $\text{CH}_4$  emissions in the TGR. During reservoir flushing, degassing would occur because of rapid depressurization and strong aeration, resulting in increased emissions of dissolved  $\text{CH}_4$  and lowering of  $\text{CH}_4$  concentration downstream [6,41]. Overall, the TGD regulated the  $\text{CH}_4$  emission regime of the Yangtze, causing dissolved  $\text{CH}_4$  to increase in the upper reach and decrease in the lower reach.

### Cause of $\text{N}_2\text{O}$ drop

$\text{N}_2\text{O}$  flux emissions over the mainstream decreased from 0.44 to 0.41  $\text{Gg N yr}^{-1}$ , and  $\text{N}_2\text{O}$  exports to the sea fell from 0.46 to 0.41  $\text{Gg N yr}^{-1}$  after TGD operation commenced. Land use changes and water quality protection measures resulted in low nitrogen loading to the TGR. Formation of hypoxia or even anoxia in the reservoir was generally restricted (Fig. 4d). The promoted denitrification, whereby  $\text{N}_2\text{O}$  was transformed directly to  $\text{N}_2$ , caused  $\text{N}_2\text{O}$  to decrease slightly upstream of the dam [42–44]. On the other hand,

riverbed scouring downstream of the TGD altered the habitat of heterotrophic denitrifiers, slowing down denitrification. This is consistent with our findings of high  $\text{NO}_3^-$  concentration but low  $\text{NO}_2^-$  concentration in the river [45] (Supplementary Figs 4 and 14a–b). Again, reservoir flushing would have raised degassing of  $\text{N}_2\text{O}$  and  $\text{N}_2$ . Discharge of cooler, high-pressure bottom water, supersaturated with gases, from the 175-m-deep reservoir to the warmer, low-pressure downstream river would enhance  $\text{N}_2\text{O}$  emissions [14]. Riverine microbial communities require phosphorus as a nutrient, and pH to regulate nitrification and denitrification processes. The estimated annual mass of reactive phosphorus retained by dams along the Yangtze was 0.5  $\text{Gmol yr}^{-1}$  in 2010, and it will rise to 2.9  $\text{Gmol yr}^{-1}$  by 2030; this would alter denitrification, thus decreasing  $\text{N}_2\text{O}$  production. Hence, the influence of phosphorus is likely to be significantly less than riverbed scouring on the nitrogen cycle downstream of the TGD. Field observations also exhibited an increase in pH downstream of the TGD since 2003; this encouraged nitrification, as evidenced by the very low levels of ammonium that were recorded (Supplementary Fig. 14).

Lastly, the key concern becomes how the enlargement of  $\text{CO}_2$  ( $1.8 \times 10^2$ – $3.4 \times 10^2$   $\text{Gg C yr}^{-1}$ ),  $\text{CH}_4$  (0.18–0.37  $\text{Gg C yr}^{-1}$ ) and  $\text{N}_2\text{O}$  (0.0072–0.01  $\text{Gg N yr}^{-1}$ ) emissions caused by the reservoir itself would be finally offset by the reduction of GHG emissions resulting from downstream habitat modification. According to pre-impoundment estimates of GHG fluxes from the reservoir and post-impoundment measurements on possible GHG pathways, such a balancing out would be expected at 766–819 km (for  $\text{CO}_2$ ), 124–180 km (for  $\text{CH}_4$ ) and 18–53 km (for  $\text{N}_2\text{O}$ ) downstream of the TGD, respectively (Fig. 5). Under the practical scenarios for TGD operation [46] (Supplementary Table 12), the overall net reduction in GHG emissions would still be significant (38.43%–44.60% for  $\text{CO}_2$ , 14.51%–19.70% for  $\text{CH}_4$  and 0.21%–2.50% for  $\text{N}_2\text{O}$ ) in the entire Yangtze. In the reservoir area, the river-valley geomorphology restricted the rise of the littoral shallow area ( $< 10$  m), resulting in less  $\text{CH}_4$  and  $\text{CO}_2$  emissions from ebullition ( $< 8\%$  in the gross GHG emission estimates of the TGR, see Supplementary Table 13). Sensitivity analysis confirmed the availability of the study results under uncertainties from the models and those induced by the TGR (Supplementary Figs 15 and 16). In the balance, the net change in GHG emissions directly caused by the TGR could alter neither the dominant GHG emission pathways from the reservoir nor the general GHG reduction trend from the

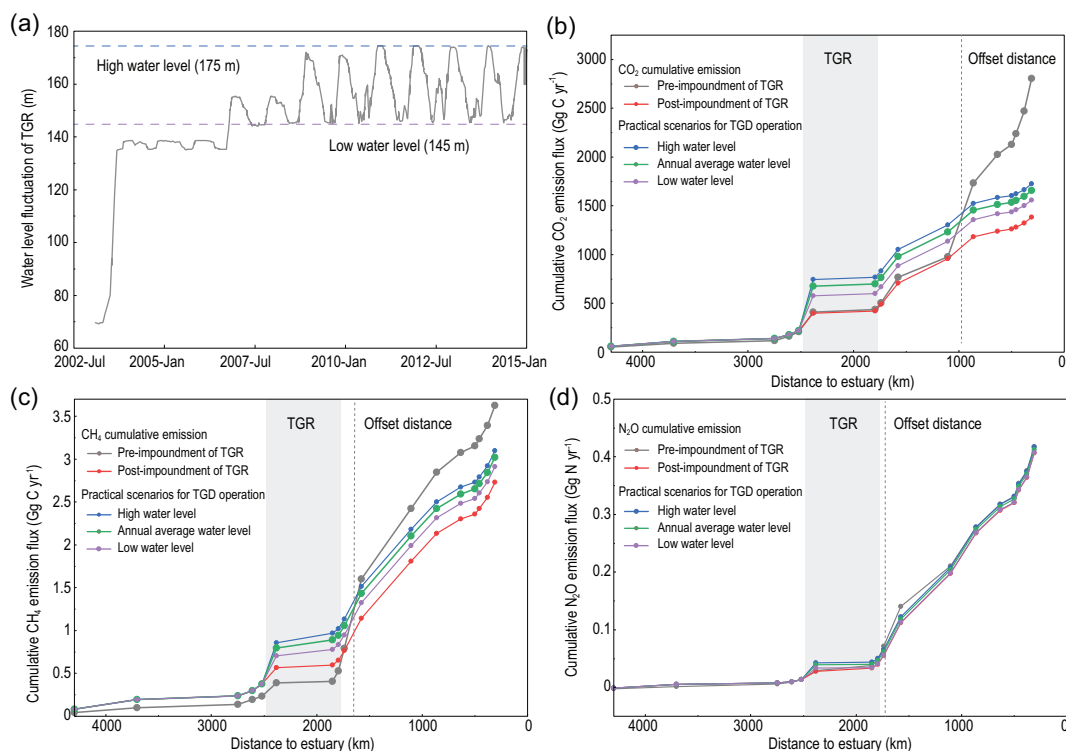


**Figure 5.** The balance of GHG emission fluxes enlarged by the reservoir itself and those reduced by habitat modification downstream from the dam under practical TGD operation. According to (a) different scenarios for the annual variation of the TGD’s operating water level, the offset distance was (b) 766–819 km for CO<sub>2</sub>, (c) 124–180 km for CH<sub>4</sub> and (d) 18–53 km for N<sub>2</sub>O downstream from the dam, respectively. Under the averaged operating water level, the vertical dotted lines indicate the locations where the changed GHG emission fluxes, due to the reservoir, were offset by the decreased GHG emissions in the downstream of the dam.

perspective of the full 4300 km along the mainstream of the Yangtze River (for details see Section 9 in the Supplementary Data).

## CONCLUSIONS

In contrast to the general claim that dams increase emissions of GHGs from rivers, we found that the TGD, the world’s largest dam, caused a significant reduction in annual average emissions of CO<sub>2</sub>, CH<sub>4</sub> and N<sub>2</sub>O over a 4300-km stretch of the Yangtze River. Meanwhile, a remarkable drop occurred in the annual export of CO<sub>2</sub> (79%), CH<sub>4</sub> (50%) and N<sub>2</sub>O (9%) to the sea from the river. These findings suggest that more profound impacts are produced by the ‘large dams’ than are expected from ‘small dams’, whose effects are limited to the vicinity of reservoirs, either spatially or temporally. The impoundment of a large reservoir not only altered the environment in the reservoir area, but also resulted in significant changes to riverine habitats downstream. In particular, long-term and long-distance riverbed erosion downstream of the large dam essentially changes the processes of photosynthesis, methanogenesis and denitrification, commencing the re-establishment of

the biogeochemical equilibrium over the whole river system. This highlights the primary importance of whole-system analysis in understanding the complex effects of large dams on readjustments of physical, chemical and biological equilibria in large rivers globally.

## METHODS

Water quality was monitored monthly at 43 hydrological stations (blue open circles, Fig. 1). Simultaneous sampling of hydrological, environmental and all GHG constituents was undertaken in the spring and autumn of 2014 along the 4300-km stretch (i.e. the actual sinuous channel length, equivalent to 2.05 times the straight-line distance of 2102 km from the start to the end of the sampling sites; red circles, Fig. 1). Further monthly sampling took place from November 2014 to September 2015 at six stations (purple solid circles, Fig. 1). Given the limited data available for model establishment (Supplementary Tables 2–3), we included data from previous studies conducted at certain sites along the Yangtze River. Details of model verification are given in Supplementary Tables 14 and 15. All samples were

collected in triplicate. Dissolved CO<sub>2</sub>, CH<sub>4</sub> and N<sub>2</sub>O were determined using the headspace equilibration technique [47]. CO<sub>2</sub>, CH<sub>4</sub> and N<sub>2</sub>O emission rates were measured using the static floating chamber technique [47,48]. CO<sub>2</sub>, CH<sub>4</sub> and N<sub>2</sub>O concentrations were obtained using a gas chromatograph.

Water chemistry monitoring was conducted by the Changjiang Water Resources Commission on a monthly basis from 1990 to 2015. pH, total alkalinity, HCO<sub>3</sub><sup>-</sup>, water temperature (T), pCO<sub>2</sub> and dissolved CO<sub>2</sub> concentrations were determined at 18 stations (Supplementary Table 16). As described in Supplementary Figs 17 and 18, ANNs based on backward propagation were used to calculate dissolved CH<sub>4</sub> (with inputs of chemical oxygen demand, dissolved oxygen, water temperature, pH, NO<sub>3</sub><sup>-</sup> and NH<sub>4</sub><sup>+</sup>) and N<sub>2</sub>O (with inputs of NH<sub>4</sub><sup>+</sup>, NO<sub>2</sub><sup>-</sup>, NO<sub>3</sub><sup>-</sup>, dissolved oxygen, water temperature and pH). The model validation of dissolved CH<sub>4</sub> and N<sub>2</sub>O concentrations (including data from previous studies conducted at certain sites along the Yangtze River) is shown in Supplementary Figs 19 and 20. Sensitivity analysis was performed by changing input variables (Supplementary Figs 15 and 16). For comparison, calculated dissolved N<sub>2</sub>O concentrations from previous regression models are listed in Supplementary Table 17. The GHG emission rate across the air–water interface was calculated using a two-layer diffusive gas exchange model [49]. Herein,  $k_{600}$  is an important parameter for calculating the gas emission rate from the dissolved gas concentration. Based on the re-examination of existing empirical formulas for  $k_{600}$  (Supplementary Table 18),  $k_{600}$  was determined for the monitoring sites at different reaches of the Yangtze River (Supplementary Table 19). Wind speed data near the hydrological stations were extracted from the China Meteorological Data Sharing Service System (<http://data.cma.gov.cn>). The atmospheric CH<sub>4</sub> concentration was assumed to be equivalent to the monthly averaged global background concentration at six monitoring stations across the world (NOAA/CMDL/CCGG air sampling network, <http://www.cmdl.noaa.gov/>). Model validation and parameter (e.g.  $k_{600}$ ) determination are detailed in the Supplementary Data.

## SUPPLEMENTARY DATA

Supplementary data are available at [NSR](#) online.

## ACKNOWLEDGEMENTS

Help with sampling and field work from Qian Chen, Meiping Tong, Huazhang Zhao, Weiling Sun, Sitong Liu, Chenyuan Dang, Tang Liu, Shufeng Liu, Can Li, Jialiang Liang, Xuan Wu and Minzheng Xie is appreciated.

## FUNDING

This work was supported by the National Natural Science Foundation of China (51721006, 92047303, and U2240205).

## AUTHOR CONTRIBUTIONS

J.R.N. designed the research. J.R.N., H.Z.W., T.M. and R.H. performed the research. H.Z.W., T.M., R.H., Z.L. and J.F.C. analyzed the data. P.C., A.G.L.B., Y.Y., B.L., Y.C.W., M.S.Z. and T.W. contributed new ideas and information. J.R.N., H.Z.W., Z.L. and Y.Y. wrote the paper with help from A.G.L.B. and P.C. All authors read, commented on and approved the final version of this article.

**Conflict of interest statement.** None declared.

## REFERENCES

- Raymond PA, Hartmann J and Lauerwald R *et al*. Global carbon dioxide emissions from inland waters. *Nature* 2013; **503**: 355–9.
- Maavara T, Parsons CT and Ridenour C *et al*. Global phosphorus retention by river damming. *Proc Natl Acad Sci USA* 2015; **112**: 15603–8.
- Barros N, Cole JJ and Tranvik LJ *et al*. Carbon emission from hydroelectric reservoirs linked to reservoir age and latitude. *Nat Geosci* 2011; **4**: 593–6.
- Hu Y and Cheng H. The urgency of assessing the greenhouse gas budgets of hydroelectric reservoirs in China. *Nat Clim Change* 2013; **3**: 708–12.
- Qiu J. Chinese dam may be a methane menace. *Nature* 2009; doi: 10.1038/news.2009.962.
- Deemer BR, Harrison JA and Li S *et al*. Greenhouse gas emissions from reservoir water surfaces: a new global synthesis. *BioScience* 2016; **66**: 949–64.
- Fearnside PM. Greenhouse gas emissions from a hydroelectric reservoir (Brazil's Tucuruí Dam) and the energy policy implications. *Water Air and Soil Poll* 2002; **133**: 69–96.
- Guérin F, Abril G and Tremblay A *et al*. Nitrous oxide emissions from tropical hydroelectric reservoirs. *Geophys Res Lett* 2008; **35**: L06404.
- Latrubesse EM, Arima EY and Dunne T *et al*. Damming the rivers of the Amazon basin. *Nature* 2017; **546**: 363–9.
- Maavara T, Lauerwald R and Regnier P *et al*. Global perturbation of organic carbon cycling by river damming. *Nat Commun* 2017; **8**: 15347.
- Maeck A, Delsontro T and McGinnis DF *et al*. Sediment trapping by dams creates methane emission hot spots. *Environ Sci Technol* 2013; **47**: 8130–7.
- Vörösmarty CJ, Meybeck M and Fekete B *et al*. Anthropogenic sediment retention: major global impact from registered river impoundments. *Glob Planet Change* 2003; **39**: 169–90.
- Graf WL. Downstream hydrologic and geomorphic effects of large dams on American rivers. *Geomorphology* 2006; **79**: 336–60.
- Fan H, He D and Wang H. Environmental consequences of damming the Lancang-Mekong River: a review. *Earth-Sci Rev* 2015; **146**: 77–91.



15. Dai Z and Liu J. Impacts of large dams on downstream fluvial sedimentation: an example of the Three Gorges Dam (TGD) on the Changjiang (Yangtze River). *J Hydrol* 2013; **480**: 10–8.
16. Ramette A and Tiedje JM. Multiscale responses of microbial life to spatial distance and environmental heterogeneity in a patchy ecosystem. *Proc Natl Acad Sci USA* 2007; **104**: 2761–6.
17. Gunkel G. Hydropower—a green energy? Tropical reservoirs and greenhouse gas emissions. *Clean Soil Air Water* 2009; **37**: 726–34.
18. Williams GP and Wolman MG. *Downstream Effects of Dams on Alluvial Rivers*. Washington: United States Government Printing Office, 1984.
19. Yang L, Qiu F and Wang X *et al.* Spatial and temporal variation of methane concentrations in the atmosphere of the Three Gorges Reservoir and its relationship with methane emissions from the reservoir (in Chinese). *Resources and Environment in the Yangtze Basin* 2012; **21**: 209–14.
20. Lo W. *Modelling Greenhouse Gas Emissions from the Three Gorges Dam*. PhD Thesis. The Hong Kong Polytechnic University, 2009.
21. Fearnside PM and Pueyo S. Greenhouse-gas emissions from tropical dams. *Nat Clim Change* 2012; **2**: 382–4.
22. Yang SL, Milliman JD and Xu KH *et al.* Downstream sedimentary and geomorphic impacts of the Three Gorges Dam on the Yangtze River. *Earth-Sci Rev* 2014; **138**: 469–86.
23. Renyong H and Jie Z. Establishment and validation of a 1-D numerical model of unsteady flow and sediment transport in the Three Gorges reservoir (TGR) (Switzerland). *Appl Mech Mater* 2013; **444–5**: 901–5.
24. Chen J, Wang F and Xia X *et al.* Major element chemistry of the Changjiang (Yangtze River). *Chem Geol* 2002; **187**: 231–55.
25. Butman D and Raymond PA. Significant efflux of carbon dioxide from streams and rivers in the United States. *Nat Geosci* 2011; **4**: 839–42.
26. Bartlett KB, Crill PM and Bonassi JA *et al.* Methane flux from the Amazon River floodplain: emissions during rising water. *J Geophys Res* 1990; **95**: 16773–88.
27. Yan W, Yang L and Wang F *et al.* Riverine N<sub>2</sub>O concentrations, exports to estuary and emissions to atmosphere from the Changjiang River in response to increasing nitrogen loads. *Glob Biogeochem Cycles* 2012; **26**: GB4006.
28. Wang Q, Koshikawa H and Liu C *et al.* 30-year changes in the nitrogen inputs to the Yangtze River Basin. *Environ Res Lett* 2014; **9**: 115005.
29. Cole JJ, Prairie YT and Caraco NF *et al.* Plumbing the global carbon cycle: integrating inland waters into the terrestrial carbon budget. *Ecosystems* 2007; **10**: 172–85.
30. St. Louis VL, Kelly CA and Duchemin É *et al.* Reservoir surfaces as sources of greenhouse gases to the atmosphere: a global estimate. *BioScience* 2000; **50**: 766–75.
31. Ran L, Lu XX and Richey JE *et al.* Long-term spatial and temporal variation of CO<sub>2</sub> partial pressure in the Yellow River, China. *Biogeosciences* 2015; **12**: 921–32.
32. Raymond PA and Cole JJ. Increase in the export of alkalinity from North America's largest river. *Science* 2003; **301**: 88–91.
33. Luo ZX, Zhu B and Zheng BH *et al.* Nitrogen and phosphorus loadings in branch backwater reaches and the reverse effects in the main stream in Three Gorges Reservoir (in Chinese). *China Environmental Science* 2007; **27**: 208–12.
34. Tan L, Cai Q and Xu Y *et al.* Survey of spring eutrophication status after 175 m experimental impoundment of Three Gorges Reservoir and comparison (in Chinese). *Wetland Science* 2010; **8**: 331–8.
35. Wang F, Wang Y and Zhang J *et al.* Human impact on the historical change of CO<sub>2</sub> degassing flux in River Changjiang. *Geochem Trans* 2007; **8**: 7.
36. Gao Q. Effects of vertical mixing on algal growth in the tributary of Three Gorges Reservoir (in Chinese). *Journal of Hydraulic Engineering* 2017; **48**: 96–103.
37. Reynolds C. What factors influence the species composition of phytoplankton in lakes of different trophic status? *Hydrobiologia* 1998; **369**: 11–26.
38. Cao M, Cai QH and Liu RQ *et al.* Comparative research on physicochemical factors in the front of Three Gorges reservoir before and after the initiate impounding (in Chinese). *Acta Hydrobiologica Sinica* 2006; **30**: 12–19.
39. Liu H, Wang Z and Lu Y. Self-adjustment mechanism of bed structures under hydrology and sediment regimes. *Hydrol Res* 2016; **47**: 136–48.
40. Guerin F, Abril G and Richard S *et al.* Methane and carbon dioxide emissions from tropical reservoirs: significance of downstream rivers. *Geophys Res Lett* 2006; **33**: L21407.
41. Li Z, Lu L and Lv P *et al.* Imbalanced stoichiometric reservoir sedimentation regulates methane accumulation in China's Three Gorges Reservoir. *Water Resour Res* 2020; **56**: e2019WR026447.
42. Lu H, Chandran K and Stensel D. Microbial ecology of denitrification in biological wastewater treatment. *Water Res* 2014; **64**: 237–54.
43. Yan X, Han Y and Li Q *et al.* Impact of internal recycle ratio on nitrous oxide generation from anaerobic/anoxic/oxic biological nitrogen removal process. *Biochem Eng J* 2016; **106**: 11–8.
44. Zhu D, Chen H and Yuan X *et al.* Nitrous oxide emissions from the surface of the Three Gorges Reservoir. *Ecol Eng* 2013; **60**: 150–4.
45. Phillips JD. Toledo Bend Reservoir and geomorphic response in the lower Sabine River. *River Res Applic* 2003; **19**: 137–59.
46. Li Z, Sun Z and Chen Y *et al.* The net GHG emissions of the China Three Gorges Reservoir: i. Pre-impoundment GHG inventories and carbon balance. *J Clean Prod* 2020; **256**: 120635.
47. Beaulieu J, Shuster W and Rebholz J. Nitrous oxide emissions from a large, impounded river: the Ohio River. *Environ Sci Technol* 2010; **44**: 7527–33.
48. Wang H, Huang R and Li J *et al.* Dissolved and emitted methane in the Poyang Lake. *Sci China Technol Sci* 2021; **64**: 203–12.
49. Weiss R and Price B. Nitrous oxide solubility in water and seawater. *Mar Chem* 1980; **8**: 347–59.